RESEARCH PAPER

COACTION PUBLISHING

Investigation of the biological properties of Cinnulin PF in the context of diabetes: mechanistic insights by genome-wide mRNA-Seq analysis

Haloom Rafehi[1,2], Katherine Ververis[1,2], Aneta Balcerczyk[3], Mark Ziemann[3], Jenny Ooi[3], Sean Hu[1,2], Faith A. A. Kwa[1], Shanon J. Loveridge[1,3], George T. Georgiadis[1], Assam El-Osta[2,3,4,5] and Tom C. Karagiannis[1,2*]

[1]Epigenomic Medicine, Baker IDI Heart and Diabetes Institute, The Alfred Medical Research and Education Precinct, Melbourne, VIC., Australia; [2]Department of Pathology, The University of Melbourne, Parkville, VIC., Australia; [3]Epigenetics in Human Health and Disease, Baker IDI Heart and Diabetes Institute, The Alfred Medical Research and Education Precinct, Melbourne, VIC., Australia; [4]Epigenomic Profiling Facility, Baker IDI Heart and Diabetes Institute, The Alfred Medical Research and Education Precinct, Melbourne, VIC., Australia; [5]Department of Medicine, Monash University, Melbourne, VIC., Australia

The accumulating evidence of the beneficial effects of cinnamon (*Cinnamomum burmanni*) in type-2 diabetes, a chronic age-associated disease, has prompted the commercialisation of various supplemental forms of the spice. One such supplement, Cinnulin PF®, represents the water soluble fraction containing relatively high levels of the double-linked procyanidin type-A polymers of flavanoids. The overall aim of this study was to utilize genome-wide mRNA-Seq analysis to characterise the changes in gene expression caused by Cinnulin PF in immortalised human keratinocytes and microvascular endothelial cells, which are relevant with respect to diabetic complications. In summary, our findings provide insights into the mechanisms of action of Cinnulin PF in diabetes and diabetic complications. More generally, we identify relevant candidate genes which could provide the basis for further investigation.

Keywords: *cinnulin PF*; *diabetes*; *diabetic complications*; *diabetic ulcer*; *mRNA-Seq*

To access the supplementary material to this article: 'Supplementary tables 1–3' please see Supplementary files under Reading Tools online.

Received: 7 November 2011; Revised: 17 January 2012; Accepted: 1 February 2012; Published: 22 February 2012

Diabetes is a highly debilitating metabolic disorder which can lead to life-threatening complications as a result of uncontrolled hyperglycemia, and is becoming an increasingly significant disease in elderly populations. Historically, many plant products have been used as treatments for diabetes, with varied success. One such plant product is cinnamon, a spice produced from the bark of trees from the genus *Cinnamomum*. Studies have shown that cinnamon has potent antioxidant and anti-inflammatory activities. *In vitro*, a 20-fold enhancement in insulin-dependent glucose metabolism following treatment with cinnamon has been shown (1). The active water soluble components of cinnamon have been identified as double-linked procyanidin type-A polymers, mainly trimers and tetramers (Fig. 1) (1). These procyanidins are naturally occurring polymers of flavonoids such as catechin which are well known to be potent antioxidants.

Water soluble components of cinnamon have been shown to result in the autophosphorylation of the insulin receptor, as well in specific inhibition of the phosphotyrosine phosphatase, which dephosphorylates the insulin

 Citation: Pathobiology of Aging & Age-related Diseases 2012, **2**: 11905 - DOI: 10.3402/pba.v2i0.11905

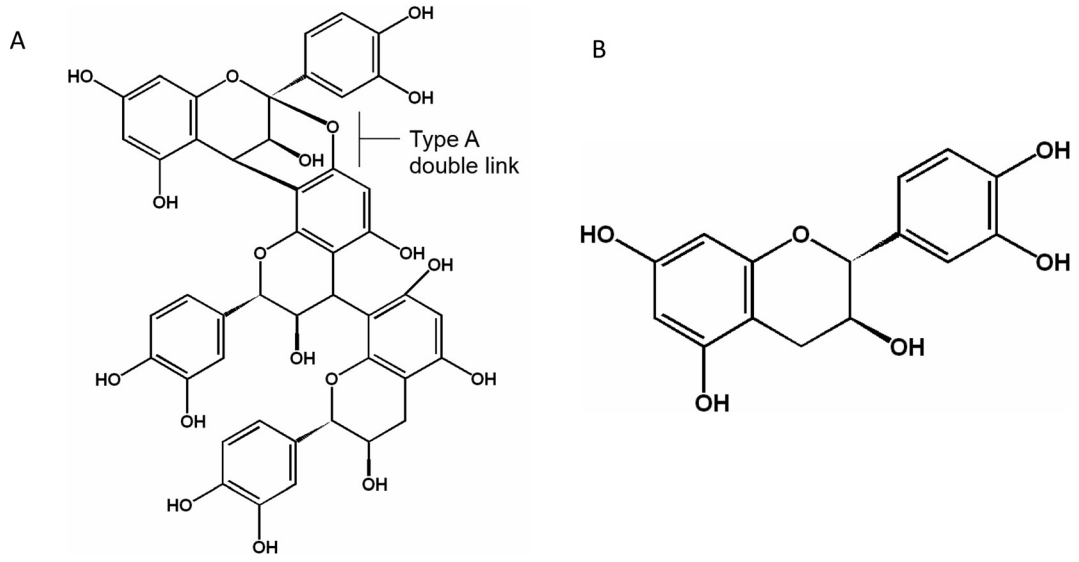

Fig. 1. Double-linked type-A procyanidin polymer (trimer) (A). Comprised of the flavanoid catechin (B), which is made up of two substituted benzene rings, and a substituted dihydropyran ring.

receptor (2). Findings from an *in vivo* study demonstrated that when an aqueous cinnamon extract was administrated orally (300 mg/kg), there was an 18% increase in phosphorylation levels of the insulin receptor-β and 33% insulin receptor substrate-1 compared to control rats (3). Overall, the findings suggested that the water soluble component of cinammon can increase insulin sensitivity, by increasing glucose uptake in skeletal muscle (3). In a clinical study, it was shown that 500 mg per day of Cinnulin PF® (CPF, a commercial cinnamon extract containing the bioactive double-linked procyanidin type-A trimers and tetramers) resulted in improvements in fasting blood sugar levels, systolic blood pressure and body composition in participants with metabolic syndrome (4).

Although there is accumulating evidence of the beneficial effects of cinnamon in diabetes, few studies have investigated the molecular mechanisms accounting for these observations. In particular, mechanisms related to the effects of cinnamon in diabetic complications are very limited. Major complications of diabetes include diabetic foot ulcers, which arise as a result of impaired wound healing in lower extremities and endothelial dysfunction which can lead to cardiovascular conditions such as atherosclerosis (Fig. 2) (5–7). The overall aim of this study was to investigate the effects of the water soluble component of cinnamon, using CPF, on gene expression changes by genome-wide mRNA-Seq analysis in representative, human keratinocyte and microvascular endothelial cell lines.

Materials and methods

Cinnulin PF preparation

The water soluble component of cinnamon bark (*Cinnamonum burmanii*), Cinnulin PF® (CPF), containing 4.5%

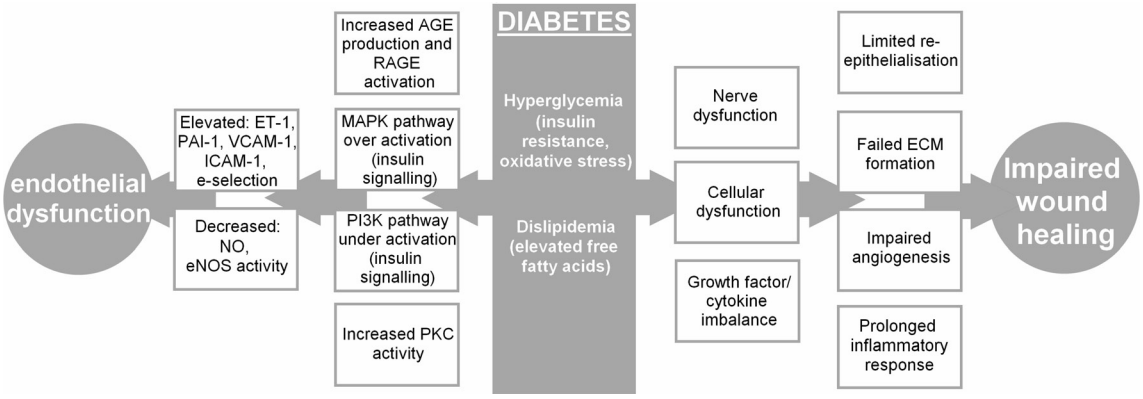

Fig. 2. The different factors which lead to impaired wound healing in diabetes.

Citation: Pathobiology of Aging & Age-related Diseases 2012, **2**: 11905 - DOI: 10.3402/pba.v2i0.11905

(page number not for citation purpose)

type-A polymers (trimeric and tetrameric) was a generous gift from Integrity Nutraceuticals International (USA). The powder was accurately weighed and dissolved in phosphate buffered saline without calcium and magnesium (PBS) by gentle rotation at room temperature for 30–60 minutes (~70% soluble). The mixture was then centrifuged for five minutes at 400 × g. The supernatant was collected, sterilized by filtration (0.22 μm) and concentrated stocks (10 mg/mL) were stored at −80°C until use.

Cell culture

Human microvasuclar endothelial, HMEC-1, cells were cultured in MCDB-131 medium (Invitrogen, Carlsbad, CA, USA), supplemented with 10% heat-inactivated fetal bovine serum (FBS), 10 ng/mL epidermal growth factor (EGF), 5000 units/L heparin, 200 μM hydrocortisone, GlutaMAX™-1 (Invitrogen) and 20 mg/mL gentamicin. Human keratinocytes (FEP-1811) were grown in keratinocyte-SFM (K-SFM) medium (Invitrogen, serum-free medium) supplemented with L-glutamine, epidermal growth factor, bovine pituitary extract and 20 mg/mL gentamicin (8). Cells were grown in a humidified 5% CO_2 environment at 37°C. As required, single cell suspensions were prepared by trypsinization (0.05% trypsin/EDTA solution, Invitrogen) for 5–10 minutes. Cell numbers were determined using a hemocytometer.

Cell viability and apoptosis

CellTiter-Blue® and ApoOne homogeneous Caspase 3/7® kits where used to examine the effects of CPF on cell viability and apoptosis, respectively, according to the manufacturer's instructions (Promega, Madison, WI, US). Cells were treated with CPF at a concentration range of 0–2048 μg/mL. Following a 24 hour incubation at 37°C, 5% CO_2, CellTiter-Blue reagent was added and incubated at 37°C, 5% CO_2 for four hours or ApoOne buffer/substrate solution was added and incubated in the dark for two hours at room temperature. Fluorescence was measured using a VICTOR 3 (PerkinElmer, Waltham MA, USA) microplate reader. The EC50 was defined as the concentration of CPF which results in 50% reduction in cell viability.

Cell cycle analysis

HMEC-1 and keratinocyte cells were treated with various concentrations of CPF (0–200 μg/mL) for 24 hours, after which cells were harvested with 0.05% trypsin, washed with PBS, resuspended in ice-cold PBS containing 2% FBS and fixed overnight with 70% ethanol by continuous rotation at 5°C. Cells were stained with an overnight incubation at 5°C in 100 μg/mL propidium iodide containing 1 μg/mL RNase A (Qiagen Inc., Valencia, CA). Samples were analyzed by flow cytometry (Facs Calibur, Becton Dickinson, Franklin Lakes, NJ, USA). Fluorescent debris were gated using forward scatter versus orthogonal side scatter and a secondary gate was placed around the single cell population using a pulse area versus pulse width dot plot. The percentage of cells in each phase of the cell cycle was analyzed using FlowJo V7.6 flow cytometry analysis software (Tree Star Inc., Ashland, OR, USA).

Migration scratch assay

HMEC-1 and keratinocytes were plated in 6-well plates. At 80% confluency and typically following a 24 hour period of supplement starvation, cells were treated with various concentrations of CPF (0–50 μg/mL) for one hour. Cells were washed with PBS and a single scratch was performed across the centre of the well using a 1 mL pipette tip. Cells were then washed twice with PBS and fresh medium was added. Digital images were acquired at defined points at the time of the scratch and after 24 hours at the same location, at a magnification of *x*4 using a camera (Olympus DP20) and light microscope (Olympus CKX4).

Total RNA isolation and cDNA synthesis

Cells were treated with CPF (20 and 100 μg/mL for keratinocytes, 20 μg/mL for HMEC-1 cells) for 24 hours. Total RNA was isolated using TRIZOL (Invitrogen). Cells suspended in TRIZOL were passed through a 21-gauge needle five times to ensure proper lysis, then RNA extraction was performed following the Qiagen protocol. Genomic DNA contamination was removed by DNAse treatment (Qiagen). First strand cDNA synthesis was performed using High-Capacity cDNA Reverse Transcription Kit (Applied Biosystems, Carlsbad, CA, USA), according to the manufacturer's instructions.

Library construction and RNA sequencing

RNAseq libraries were prepared according to Illumina mRNAseq library preparation kit (Illumina Inc. San Diego, CA, USA, cat # RS-100-0801). Briefly, 8 μg of total RNA was taken for mRNA isolation using poly-T oligo-attached magnetic beads. Poly-A mRNA was fragmented with the presence of divalent cations under elevated temperatures. The mRNA fragments were reverse transcribed via SuperScript II (Invitrogen) with random primers. The second strand was synthesized with addition of RNaseH and DNA Pol I. Double stranded complementary DNA (cDNAs) were end-repaired, followed by 3′ adenylation using Klenow fragment (3′ to 5′ exo minus). Then Illumina paired end adapters with T- overhangs at their 3′ end were ligated to the cDNAs. Following column purification (Qiagen MinElute), to remove excess of unligated adapter, library cDNA was separated on a 2.0% agarose gel. Library cDNA in the range of 200 bp ± 10 bp fragments were isolated by gel purification (Qiagen) and amplified with 15 cycles of Phusion DNA polymerase mediated PCR (10s 98°C, 30s

65°C, 30s 72°C) using oligonucleotides complementary to Illumina sequencing adapters. Column purified libraries were quantified fluorometrically (Invitrogen), and visualised by MultiNA (DNA 2500 kit) electrophoresis for quality assurance. Libraries were diluted to 10 nM and stored at −20°C prior to cluster generation. Denatured DNA samples were diluted to 6 pM prior to cluster generation (v4 cat # GD-103-4001). Flow cell sequencing of 36 bp tags was conducted on a Genome Analyzer II apparatus (Illumina) according to the manufacturer's protocols using v4 sequencing reagents (cat # FC-104-4001).

Quantitive reverse transcriptase PCR (qPCR)

PCR amplification was performed using an Applied Biosystems 7500 Fast Real-Time PCR System. Primers used in the validation were HPRT-1 (F: TGACACTGG CAAAACAATGCA, R: GGTCCTTTTCACCAGCAA GCT), HMOX-1 (F: TCCCCTCGAGCGTCCTCAGC, R: TGGGGCATGCTGTCGGGTTG), VEGFA (F: TGAG GAGTCCAACATCACCA, R: TCTCTCCTATGTGC TGGCCT), VEGFB (F: CCACCAGAGGAAAGTGG TGT, R: ATGAGCTCCACAGTCAAGGG), CASP-1 (F: CCACAATGGGCTCTGTTTTT, R: CATCTGG CTGCTCAAATGAA), JUNB (F: CACCTCCCGTT TACACCAAC, R: GGAGGTAGCTGATGGTGGTC), JUND (F: CGCCTGGAAGAGAAAGTGAA, R: GTT GACGTGGCTGAGGACTT), MMP1 (F: CAGAGGG AGCTTCCTAGCTG, R: AGTGGAGGAAAGCTGTG CAT), SOD-2 (F: CAGTGTGCGGCACCAGCAGG, R: TGAGGTTCCAGGGCGCCGT), ICAM-1 (F: GGC CACGCATCTGATCTGTA, R: CACTTCCCCTCTCA TCAGGC), p50 (F: ACTGCCAACAGCAGATGG CCCA, R: GCACCAGGTAGTCCACCATGGG). 5 pmoles of forward and reverse primer, cDNA template and FAST SYBR® Green Master Mix (Roche, Indianapolis, IN, USA) were mixed to a final volume of 20 µl. Reactions were incubated at 95°C for 10 min, followed by 40 cycles of 95°C for 10 s and 60°C for 30 s. Analyzed genes were normalized to the level of HPRT1.

Analysis

Sequencing was performed at a depth of ∼20 million mapped reads per sample. The number of sequence reads and alignment statistics are shown in Table 1. Reads generated by the Illumina base calling software V1.6 were aligned with Burrows Wheeler Aligner to the human transcriptome database curated by RefSeq (Hg18 build). Raw counts were normalised to adjust for slightly differing data volume across lanes giving the widely used score reads per transcript per million reads. These scores were used to determine relative fold changes and the conventionally used ±1.5 fold-change, which is discernable with qRT-PCR was defined a significant change in expression. The online program MetaCore (GeneGo Inc. St. Joseph, MI, USA) was used for pathway analysis. GeneGo is a commercial pathway analysis package however those interested can further investigate pathways discussed in this manuscript using freely available packages such as DAVID functional annotation tools (http://david.abcc.ncifcrf.gov/tools.jsp).

Data is expressed as the mean±SD, and where relevant, statistical analysis was performed using a one-way Anova followed by a Dunnett's test where $*p < 0.05$ was considered statistically significant.

Results

CPF induces a dose-dependent decrease in cell viability and increased apoptosis in HMEC-1 and keratinocytes

The effect of CPF on cell viability and induction of apoptosis in HMEC-1 and keratinocyte cells was assessed using the CellTiter-Blue and ApoOne Homogeneous Caspase 3/7 assay kits (Fig. 3). The findings indicate that CPF induces a dose-dependent decrease in cell viability in both cell lines. The EC50 values were calculated to be 416 and 663 µg/mL for HMEC-1 and keratinocyte cells, respectively (Fig. 3A,B). Similarly, the caspase activity data indicated a concentration-dependent increase in apoptosis in both HMEC-1 and keratinocytes (Fig. 3C,D). The effect of CPF on the cell cycle was accessed using PI staining and FACS analysis. Cell cycle analysis indicated that CPF had minimal effects on the different stages of the cell cycle, except for the increase seen in the percentage of cells in the sub-G1 population in both cell lines at 100 and 200 µg/mL (Fig. 4).

Table 1. Sequence reads and alignment statistics for mRNA-seq experiments

	HMEC-1		Keratinocytes		
	Untreated	CPF 20 µg/mL	Untreated	CPF 20 µg/mL	CPF 100 µg/mL
Total reads	27500928	24518899	24780637	27716895	27984648
Mapped reads	22554037	20981983	20517834	23152109	22764111
% aligned	82.0	85.6	82.8	83.5	81.3

Citation: Pathobiology of Aging & Age-related Diseases 2012, **2**: 11905 - DOI: 10.3402/pba.v2i0.11905

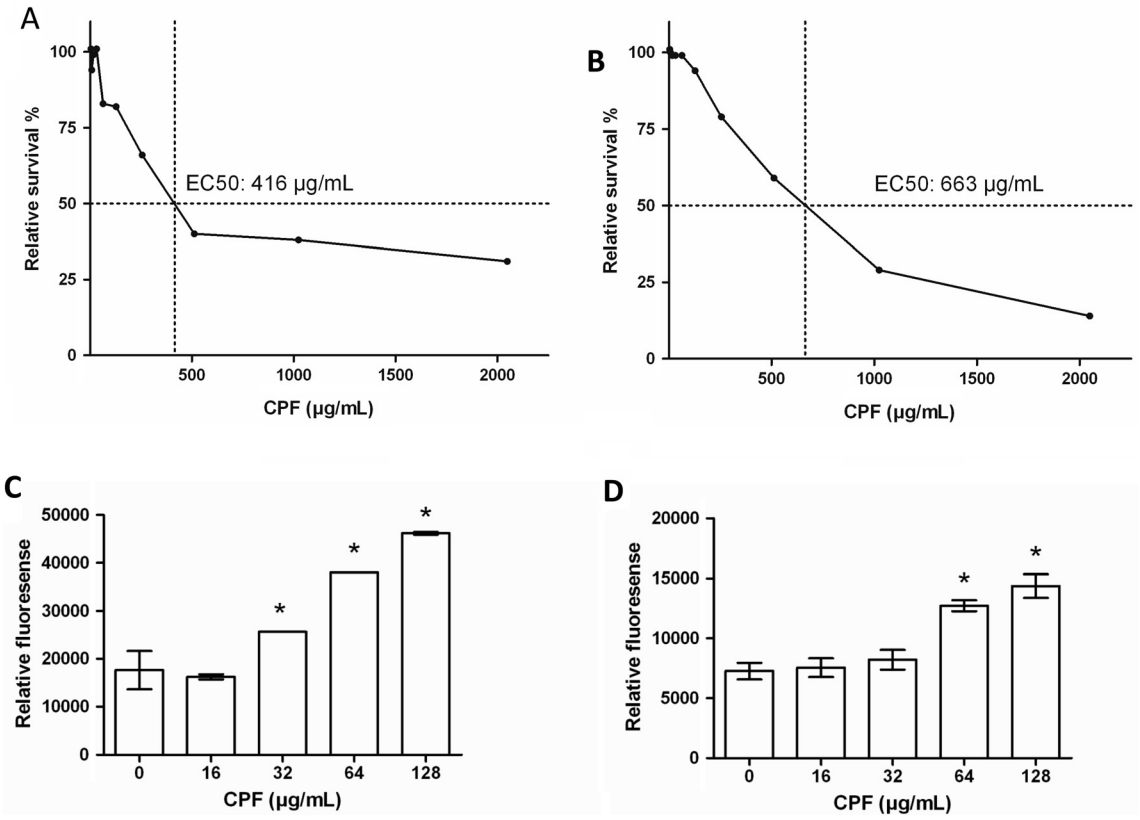

Fig. 3. Cell viability and apoptosis. Graphs showing the relative survival and EC50 (µg/mL) values following 24 hour incubations with CPF (0, 1, 2, 4, 8, 16, 32, 64, 128, 256, 512, 1024 µg/mL), in HMEC-1 (A) and keratinocytes (B) using the CellTiter-Blue® Assay. The results of the ApoOne homogeneous 3/7® assay indicating caspase activity in HMEC-1 (C) and keratinocytes (D) cells treated with various concentrations of CPF for 24hrs. The data is representative of at least two independent experiments and is presented as the mean ± SD of triplicate determination from a single experiment. *indicates $p < 0.05$, compared to the control.

CPF enhances migration at 20 µg/mL in both HMEC-1 and keratinocytes

To determine the effect of CPF on cell migration *in vitro*, a scratch migration assay was used in HMEC-1 and keratinocytes. It was found that in both cell lines, CPF promoted cell migration at the lower concentrations investigated compared to the untreated controls following a one hour treatment and 24 hour incubation, with the effect being most profound at 20 µg/mL in both the HMEC-1 cells and keratinocytes (Fig. 5). However, CPF was not effective at promoting cell migration at higher concentrations.

CPF alters the expression levels of a finite number of genes

To determine the effect of CPF on genome-wide gene expression, mRNA sequencing was performed by next generation sequencing (NGS), using keratinocytes treated at 20 and 100 µg/mL and HMEC-1 cells treated at 20 µg/mL for 24 hours; gene expression levels were compared to the relevant untreated controls. The 20 most up and down regulated genes for each treatment group is indicated in Table 2 and more detailed characteristics of each of the genes are described in supplementary Tables 1–3. The mRNA-Seq findings indicate that the greatest changes in genes expression levels was found in keratinocytes treated with 100 µg/mL CPF, with 8% percent of genes up regulated and 11% down regulated (Fig. 6A). By comparison, 4% of genes were up regulated and 3% down regulated in keratinocytes treated with 20 µg/mL, and 6% up regulated and 5% down regulated in HMEC-1 cells treated with 20 µg/mL CPF (Fig. 6A). A comparison of the mRNA-Seq data for the two cell lines indicated that there was very little overlap between the genes up and down regulated in keratinocyte and HMEC-1 cells treated with 20 µg/mL CPF (Fig. 6Bi). As expected a large overlap was observed between the up and down regulated genes for the low and high CPF concentrations in keratinocytes however, there are certain genes which are up or down regulated at 20 µg/mL which are either unchanged at 100 µg/mL or regulated in the opposite direction (Fig. 6Bii). RT-PCR was used to validate mRNA-Seq findings and positive correlation was identified for validated genes (Fig. 7).

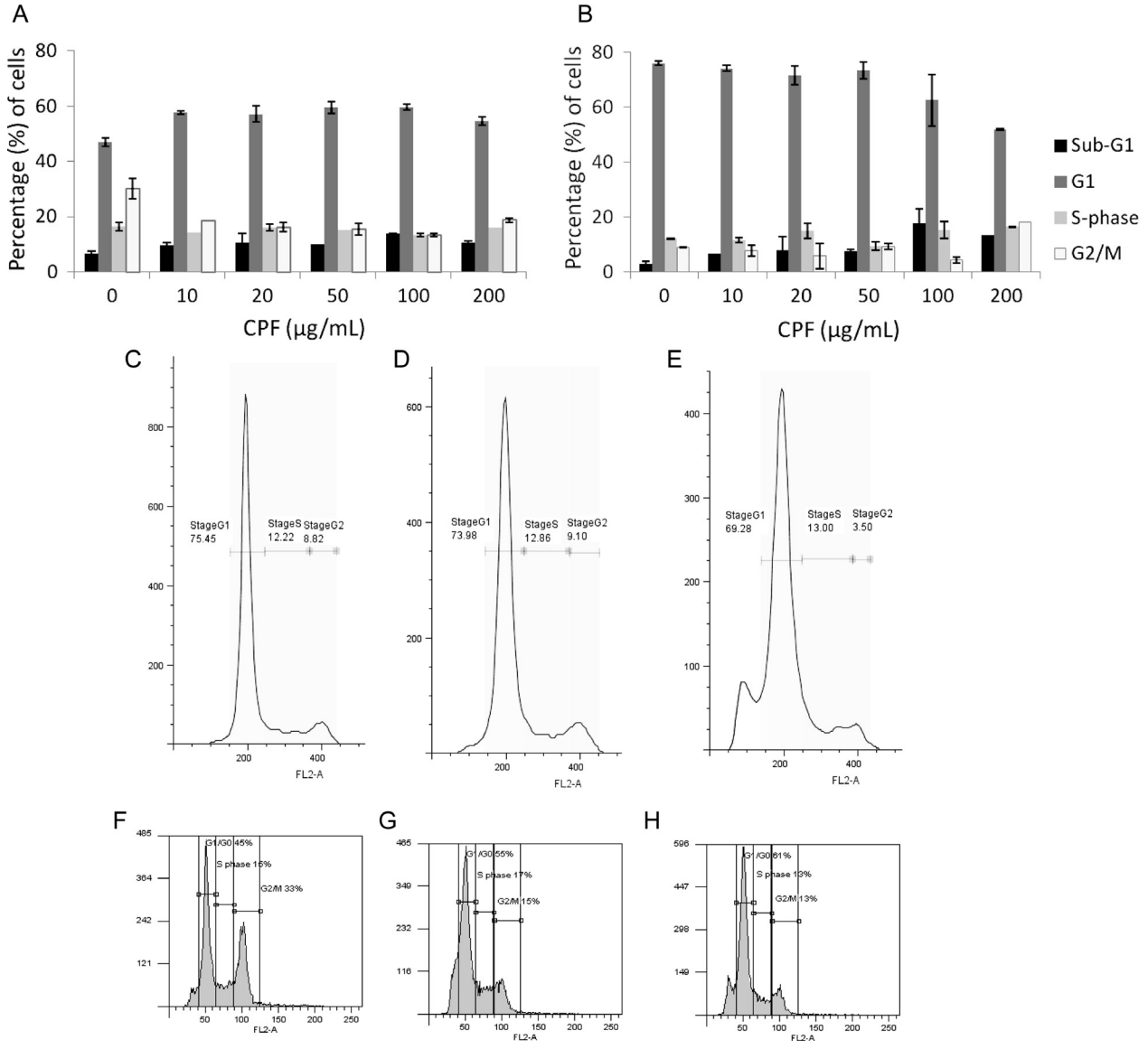

Fig. 4. Graph showing the average % of cells in the different phases of the cell cycle in HMEC-1 cells (A) and keratinocyte cells (B). Cells were incubated with CPF for 24 hours, fixed and stained with propidium iodide. The proportion of cells in the different stages of the cell cycle was determined by FACS analysis. The data is representative of two independent experiments and is expressed as the mean ± SD from a single experiment performed in duplicate. C–E show graphs of the cell cycle distribution of keratinocyte cells and F–H HMEC-1 cells treated with CPF at 0 (C, F), 20 (D, G) and 100 (E, H) µg/mL.

CPF alters the expression of genes related to the cell cycle, DNA replication and repair and apoptosis at a high concentration

Down regulation of genes involved in cell cycle regulation, DNA replication and repair was seen in keratinocytes treated with 100 µg/mL of CPF (Table 3). For example, there was extensive down regulation of cyclins and cyclin dependent kinases, which are proteins essential for the regulation of the different stages of the cell cycle. Further, down regulation of important DNA replication genes such as DNA polymerase and topoisomerase were also observed. Down regulation of genes such as BRCA-1 and p53 results in impaired DNA repair. There was also a corresponding increase in genes involved in apoptosis. For example, BAX is involved in initiating the mitochondrial apoptotic pathway, while BIM, BIK and PUMA block proteins required for normal mitochondrial function (Table 3).

CPF alters the expression of genes involved in proliferation, migration and wound healing at 20 µg/mL in both HMEC-1 and keratinocytes

Up regulation of genes involved in proliferation and cellular migration was observed in both HMEC-1 cells and keratinocyte cells treated with 20 µg/mL CPF (Table 4). For example, in keratinocytes there is up

Citation: Pathobiology of Aging & Age-related Diseases 2012, **2**: 11905 - DOI: 10.3402/pba.v2i0.11905

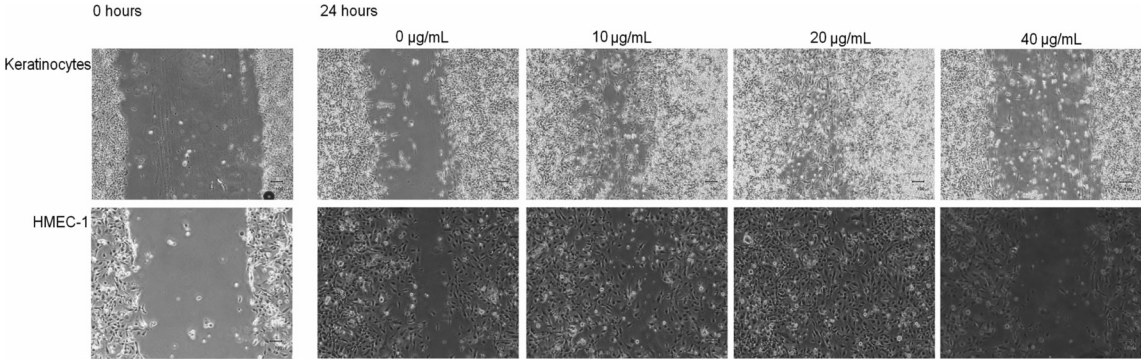

Fig. 5. CPF promotes cell migration at low concentrations. Images are of keratinocytes (top) and HMEC-1 cells (bottom) treated with various concentrations of CPF (0, 10, 20 and 40 µg/mL) for 1 hour. Scratches were performed immediately following the incubation and images were taken at 0 hrs (representative images shown) and 24 hrs post scratching; magnification ×4. Data is representative of five independent experiments for keratinocytes and two independent experiments for HMEC-1.

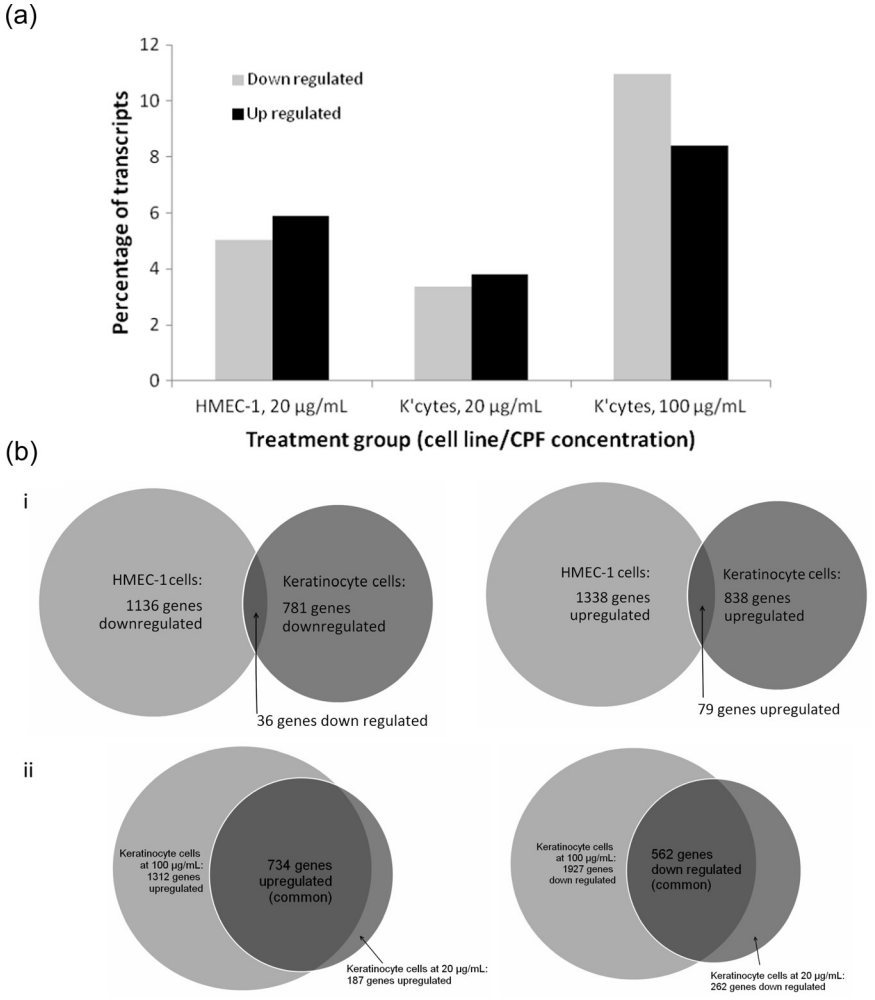

Fig. 6. (A) The% of transcripts up/down regulated for the three treatment groups. HMEC-1 cells were incubated with 20 µg/mL CPF and keratinocytes were incubated with 20 and 100 µg/mL for 24 hours. Significant gene changes were based on a fold change of ±1.5 compared to the relevant untreated control. (B) Venn diagrams showing the number of genes up and down regulated in HMEC-1 and keratinocyte cells treated with CPF (20 µg/mL) for 24 hours (i) and in keratinocytes treated with 20 and 100 µg/mL CPF for 24 hours (ii).

Table 2. The top 20 most up/down regulated genes by CPF in the three treatment groups

Keratinocytes 20 μg/mL			Keratinocytes 100 μg/mL			HMEC-1 20 μg/mL		
UP	Gene	Fold change	UP	Gene	Fold change	UP	Gene	Fold change
1	TM4SF19	18.15	1	TM4SF19	41.71	1	CRYAB	15.93
2	G0S2	7.06	2	NDRG1*	26.86	2	CRLF1	11.42
3	NDRG1*	6.6	3	KRT17	21.93	3	PTGDS	6.11
4	NDRG1*	5.72	4	GDF15	15.6	4	SOX18	5.93
5	IL6	4.97	5	HMOX1	15.22	5	BCYRN1	5.51
6	ITGA2	4.81	6	S100P	13.79	6	MIR762 (includes EG:100313837)	5.37
7	RELB	4.74	7	SAT1*	12.31	7	FOS	5.25
8	MALL	4.59	8	ITGA2	12.27	8	ID1*	4.88
9	GPR109A	4.51	9	G0S2	11.54	9	PGF	4.77
10	TLR2	4.26	10	TRIB1	10.69	10	TRNP1	4.36
11	LAMB3*	3.88	11	TLR2	10.46	11	SYT15*	4.19
12	BHLHE40	3.87	12	AREG	10.4	12	FBLN5	3.89
13	SAA1*	3.72	13	ATF3*	9.8	13	C4ORF48*	3.8
14	LAMC2*	3.7	14	LCN2	9.73	14	SNORD36B	3.76
15	COL6A2*	3.69	15	FABP3	8.72	15	SNORD114-3	3.76
16	LAMB3*	3.69	16	LAMB3*	8.41	16	JUNB	3.72
17	AREG	3.65	17	ATF3*	8.11	17	LYL1	3.52
18	LAMB3*	3.64	18	HSD17B14	7.99	18	HCN2	3.52
19	KRT17	3.59	19	SOD2*	7.82	19	HES4*	3.5
20	LAMC2*	3.57	20	DHDH	7.77	20	METRN	3.44
DOWN			DOWN			DOWN		
1	TNNI2*	−8.91	1	ALPP	−14.99	1	SNORD84	−5.58
2	TNNI2*	−8.46	2	HPDL	−13.57	2	RN18S1	−4.92
3	SYT8	−8.24	3	C10ORF114	−12.24	3	RN7SK	−4.91
4	H19	−6.05	4	MIR675 (includes EG:100033819)	−10.4	4	RMRP (includes EG:6023)	−4.78
5	SNORD96A (includes EG:619571)	−6.02	5	H19	−10.14	5	SNORD81	−4.65
6	TNNI2*	−5.8	6	PROM2*	−8.04	6	MIR1978	−4.52
7	ANKRD2*	−5.78	7	IGFBP3*	−7.94	7	SNORA11	−4.03
8		−5.28	8	SNORD31	−6.66	8	APLN	−3.96
9	MIR663B	−5.21	9	TMEM139	−6.64	9	SCARNA9L	−3.84
10	MIR675 (includes EG:100033819)	−4.98	10	PDLIM2*	−6.12	10	SNORD14D (includes EG:85390)	−3.72

Table 2 (Continued)

Keratinocytes 20 μg/mL			Keratinocytes 100 μg/mL			HMEC-1 20 μg/mL		
UP	Gene	Fold change	UP	Gene	Fold change	UP	Gene	Fold change
11	MESP1	−4.83	11	PLCB4*	−5.86	11	SNORD38A (includes EG:94162)	−3.72
12	SULT1E1	−4.81	12	UPK3B*	−5.65	12	RN28S1	−3.58
13	SNORA57	−4.64	13	FAM46B	−5.62	13	SNORD35B	−3.49
14	RNU2-1	−4.29	14	RHPN1	−5.55	14	TMEM100*	−3.44
15	MIR492	−4.29	15	MIR663B	−5.55	15	SCARNA9 (includes EG:619383)	−3.42
16	FOS	−4.09	16	PDLIM2*	−5.53	16	RNY4	−3.41
17	FGD3*	−4.06	17	WNT7A	−5.5	17	MALAT1	−3.39
18	AGR2	−3.99	18	FZD2	−5.43	18	SNORD110 (includes EG:692213)	−3.35
19	GMPR	−3.98	19	ID3	−5.38	19	SNORD102	−3.26
20	MIR762 (includes EG:100313837)	−3.95	20	MGC16121	−5.31	20	SNORD16	−3.1

regulation of the genes expressing the EGF-R ligands amphiregulin and HB-EGF. In HMEC-1 cells, there was up regulation of the transcription factors c-FOS and c-JUN, as well as PDGF-B. Also, in keratinocytes up regulation of genes involved in migration, including integrins, amphiregulins and HB-EGF was observed. In HMEC-1 cells, genes changes associated with migration included the up regulation of PDGF-B and integrins (Table 4).

Further, changes in the expression of inflammation-associate genes were observed in both HMEC-1 and keratinocytes treated with 20 μg/mL CPF (Table 4). TGF-β1 was up regulated in HMEC-1 cells while the receptor was also up regulated in keratinocyte cells at 20 μg/mL. While production of IL-6 was increased in keratinocyte cells, it was decreased in HMEC-1 cells. CCL2 (macrophage chemotactic protein) was also down regulated in HMEC-1 cells. In addition, a number of gene expression changes were observed in both cell lines at 20 μg/mL CPF which may be beneficial for the promotion of wound healing (Table 4). For example, in HMEC-1 cells there was up regulation of TIMPs, with a corresponding, general decrease in MMP expression levels, which is important for extracellular matrix formation and re-epithelialisation. There was also up regulation of genes involved in angiogenesis, including PDGF-B in HMEC-1 cells, and HIF-1α and VEGF in keratinocytes (Table 4).

CPF induces changes in the expression of genes related to endothelial cell function

Up regulation of superoxide dismutase was observed in keratinocyte cells (Table 4). In HMEC-1 cells the expression of numerous genes which may be either detrimental or beneficial to endothelial cell function was following treatment with 20 μg/mL CPF. Beneficial changes include the upregulation of eNOS, while potentially detrimental changes include the up regulation of genes encoding for endothelin-1, protein kinase C and PAI-1 (Table 4).

Discussion

We investigated the effects of a water soluble cinnamon extract, CPF, in the context of diabetic complications, by examining gene expression changes in human keratinocytes and HMEC-1 cells by mRNA-Seq. When examining the mRNA-Seq data it is important to consider that the main aim of this study was to identify potential gene targets for further investigation. Much of the following discussion is speculative on the basis of the gene expression analysis in the context of diabetic complications. Only changes in gene expression and not the functional endpoint of gene expression – i.e. synthesis of a functional protein, post-translational modifications – were examined in this study. Further issues when using crude extracts are related to modifications which occur *in vivo* (e.g. conjugation reactions) and bioavailability of the

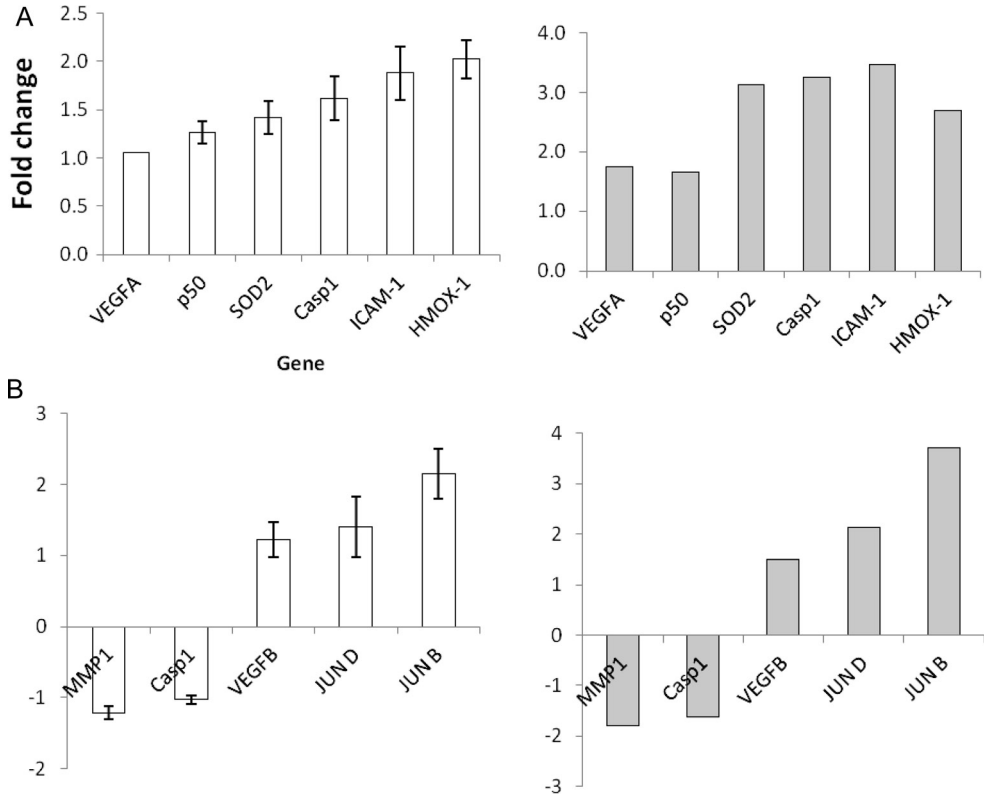

Fig. 7. RT-PCR (white, left) was used to validate the mRNA-Seq results (grey, right). Keratincoye (A) and HMEC-1 (B) cells were treated with 20 μg/mL CPF for 24 hours. RNA was then isolated from the cells, and the RNA of a selected number of genes was then amplified by RT-PCR. The results are expressed as the fold change in mRNA expression compared to untreated cells. RT-PCR results represent the mean ± SD from a single experiment performed in triplicate.

active components in cells. The uptake of polyphenolic compounds have been examined in numerous studies, and a number of studies have investigated the effects various cinnamon extracts in cell culture systems indicating the intracellular absorption of relevant compounds (9–14). In this context, *in vivo* bioavailability is also an important consideration. Although studies have reported that procyanidins are bioavailable in rodents and humans, the issue remains largely controversial and requires further exploration.

Our initial experiments indicate that CPF promotes migration at concentrations between 10 and 20 μg/mL in both keratinocytes and HMEC-1 cells (Fig. 4). Although we performed detailed time-course studies, using cell viability, apoptosis and migration, we specifically chose to closely investigate treatment with 20 μg/mL at 24 hours to reflect a non-toxic/non-apoptotic concentration of the formulation in both cell lines. mRNA-Seq analysis indicated that numerous genes associated with diabetic wound healing were regulated by CPF (Table 4). For example, certain integrins which are transmembrane glycoproteins involved in cell migration by interacting with components of the extracellular matrix such as laminin 1, fibronectin and collagen (types I, II and IV), were up regulated by CPF in both cell lines. Further, platelet derived growth factor B (PDGF-B) was up regulated 2.18 fold in HMEC-1 cells and fibroblast growth factor-2 (FGF-2) was found to be increased 1.75 fold in keratincoytes treated with 20 μg/mL CPF (Table 4). FGF-2 has been shown to induce keratinocyte migration *in vitro* and has also been strongly associated with promoting angiogenesis (15). Other proteins involved in migration pathways that were found to be up regulated by CPF include CDC42, Fyn and PAK1. Furthermore, up regulation of the epidermal growth factor receptor (EGF-R) ligands amphiregulin and heparin binding epidermal growth factor (HB-EGF) in keratinocyte cells.

An aspect which leads to impaired diabetic wound healing is the prolonged inflammatory phase which prevents the progression of the healing process. This is associated with decreased expression of cytokines, including IL-10, IL-6, TGF-β1 and receptors TGF-βR-I and TGF-βR-II (16–19). It was found that CPF increased the expression of TGF-β1 in HMEC-1 cells but not in keratinocytes. Furthermore, TGF-βR-I mRNA expression was increased in keratinocyte cells treated with 20 μg/mL CPF, while expression of both receptors was decreased in HMEC-1 cells (Table 4).

Citation: Pathobiology of Aging & Age-related Diseases 2012, **2**: 11905 - DOI: 10.3402/pba.v2i0.11905

Table 3. Regulation of genes involved in DNA replication and repair, the cell cycle and apoptosis, following treatment of keratinocytes and HMEC-1 cells with CPF

		HMEC-1	Keratinocytes	
Process	Gene	20 μg/mL	20 μg/mL	100 μg/mL
DNA replication	DNAPol ε			−2.29
	DNAPol α			−3.07
	PCNA			−1.51
	TOP2	−1.56		−1.81
	FEN1			−2.09
	DNA ligase 1			−1.92
Cell cycle	Cyclin A			−2.59
	Cyclin B			−2.87
	Cyclin D	1.61		−2.05
	Cyclin E			
	APC	1.68	−1.76	−1.77
	CDK1 [p34]		−1.51	−2.35
	CDK2			−1.86
	CDK4			
	CDK6		1.67	
	E2F1			−2.63
	E2F2			−2.13
	DP1			−1.87
	CDC25A			−2.03
	CDC25B			
	CDC25C			−1.6
	Aurora A			−2.2
	Aurora B			−2.95
	p21		2.07	5.34
	GADD45α		1.74	2.92
	GADD45β	1.76	−1.96	−3.07
DNA repair	p53			−1.83
	BRCA1			−1.77
	ATM			
	ATR	−1.57		
	PARP-1			−2.3
Apoptosis	FasR (CD95)			1.76
	Caspase 3	−1.52		
	Caspase 7	−1.3		
	BAX			1.75
	BIM			1.6
	PUMA			3.56
	BIK			5.57
	BCL-XL			1.7
	NOXA	−1.78		2.66

Further, extracellular matrix (ECM) formation is impaired in diabetic wound healing and increased expression of matrix metalloprotienases (MMPs) has been implicated (20). Although the expression of most MMPs was not changed, expression of MMP-1 and MMP-14 were both down regulated in HMEC-1 cells (Table 4). This was associated with a corresponding increase in the expression of some tissue inhibitors of MMPs (TIMPs) in HMEC-1 cells. Angiogenesis, a process which is essential for wound healing and the delivery of nutrients and oxygen to the newly forming and highly active granulation tissue, is also impaired in diabetes. One reason for this is the decreased expression of hypoxia inducible factor-1-alpha (HIF-1α) in response to glucose. HIF-1α leads to the production of growth factors needed for angiogenesis such as vascular

Table 4. The fold change of the expression of mRNA in genes involved in various processes, following treatment of keratinocytes and HMEC-1 cells with CPF

		HMEC-1	Keratinocytes	
Process	Gene	20 μg/mL	20 μg/mL	100 μg/mL
Proliferation	c-FOS	5.25	−4.09	−3.82
	c-JUN	1.61		1.93
	AKT(PKB)		1.63	2.18
	ERK1/2	1.66		1.73
Cell migration	PDGF-B	2.18		−2.23
	Fyn		1.67	2.09
	CDC42		1.56	1.66
	PAK4		1.8	
	α2β1 integrin		4.81	12.27
	α4β1 integrin		1.64	1.64
	α5β1 integrin	2.1	2.55	4.28
	α4β7 integrin		1.64	
	ITGA-5	2.1	2.55	4.28
	FGF-2		1.75	
	FGF-5			2.02
	Amphiregulin		3.65	10.4
	HB-EGF		1.62	5.93
Anti-inflammatory	TGF-β1	1.98		
	TGF-β2		−1.58	
	TGF-βR-I	−1.55	1.52	1.9
	TGF-βR-II	−1.7		
	IL-6	−2.24	4.97	5.03
Wound healing (general)	TIMP-1	1.78		
	TIMP-2	1.61		1.96
	TIMP-3	1.7		
	MMP-1	−1.82		
	MMP-14	−1.59		
	MMP-15	1.76		
	LAMA3		3.88	8.41
	CCL2	−1.89		
	HIF-1α	−1.62	2.18	1.97
	PDGF-B	2.18		−2.23
	IL-8	−1.69		
	VEGF-A		1.74	3.79
	VEGF-B	1.5		
	VEGF-C		2.27	2.13
Antioxidant enzymes	SOD2		3.12	7.82
	PRDX2			−1.74
Endothelial dysfunction	eNOS	3.1		
	ET-1	1.75		
	PAI-1	1.86		
	ICAM-1		3.47	3.86
	IL-6	−2.24	4.97	5.03
	Leptin R	−2.8		2.14
	RAGE		−1.52	1.5
	PKC	1.68	1.69	1.77
	Erk (MAPK1/3)	1.66		1.73
	MAP2K2	1.7		
	PI3K	−1.8		2.33

Citation: Pathobiology of Aging & Age-related Diseases 2012, **2**: 11905 - DOI: 10.3402/pba.v2i0.11905

endothelial growth factor (VEGF) (21, 22). CPF may improve angiogenesis by increasing HIF-1α expression in keratinocytes and by the up regulation of VEGF-A, VEGF-B and VEGF-C observed in the cell lines (Table 4).

Endothelial dysfunction involves the altered phenotype of endothelial cells as a result of a number of factors including decreased bioavailability of nitric oxide (NO), increased oxidative stress, a pro-inflammatory environment and increase in prothrombotic factors (23). In the endothelium, NO is produced by endothelial NO synthase (eNOS). It plays an important role in normal vascular homeostasis and vasodilation and is helps to protect the blood vessels from endogenous injury by mediating a number of events. For example, eNOS prevents leukocyte and platelet interaction with the endothelial cells and inhibits VSMCs from proliferating and migrating (24–26). In endothelial dysfunction, NO is degraded by ROS, and activation of the RAGE receptor by increased AGE levels, resulting in decreased eNOS activation. Although CPF lead to an increase in the expression of the antioxidant enzyme superoxide dismutase (SOD) in keratinocytes and decreased expression of RAGE, the same effects were not observed in HMEC-1 (Table 4). However, eNOS expression in HMEC-1 cells was increased, which could potentially lead to increased expression of NO.

It should be noted that CPF also increased the expression of a number of genes which could promote endothelial dysfunction for example, endothelin-1 (ET-1), a potent vasoconstrictor up-regulated in diabetes. Further, insulin resistance results in the up regulation of plasminogen activator inhibitor type-1 (PAI-1) and adhesion molecules such as VCAM-1, ICAM-1 and E-selectin via the MAPK pathway, which may contribute to endothelial dysfunction (27, 28). CPF did not alter the expression of the adhesion molecules however there was an increase in the expression of PAI-1. Furthermore, up regulation of a number of proteins involved in the MAPK pathway in HMEC-1 cells – MAPK1/3 and MAP2K2 – which is already up regulated in the diabetes, was observed.

Overall, our findings may provide some insights into the mechanisms of action of the water soluble cinnamon extract, CPF, in the context of diabetic complications. Our sequencing data provides numerous gene targets which will provide the basis for further interrogation. Finally, this study was performed in transformed human cell lines in normoglycemic conditions and further experimentation will incorporate the use of normal cell lines and hyperglycaemic conditions. Our analysis is comprehensive with respect to diabetic wound healing and further examination in cell culture systems will involve the use of other relevant cell lines such as fibroblasts and cells of the immune system. Given limitations associated with cell culture studies further it is preferable that further studies are conducted using appropriate *in vivo* models and isolation of relevant cells for analysis.

Acknowledgements

The support of the Australian Institute of Nuclear Science and Engineering is acknowledged.

Conflict of interest and funding

TCK was the recipient of AINSE awards. Epigenomic Medicine and Human Epigenetics Labs are supported by the National Health and Medical Research Council of Australia. HR is supported by an Australian post-graduate and Baker IDI bright spark awards. KV is supported by a Baker IDI post-graduate scholarship. Supported in part by the Victorian Government's Operational Infrastructure Support Program.

References

1. Anderson RA, Broadhurst CL, Polansky MM, Schmidt WF, Khan A, Flanagan VP, et al. Isolation and characterization of polyphenol type-A polymers from cinnamon with insulin-like biological activity. J Agric Food Chem 2004; 52: 65–70.
2. Imparl-Radosevich J, Deas S, Polansky MM, Baedke DA, Ingebritsen TS, Anderson RA, et al. Regulation of PTP-1 and insulin receptor kinase by fractions from cinnamon: implications for cinnamon regulation of insulin signalling. Horm Res 1998; 50: 177–82.
3. Qin B, Nagasaki M, Ren M, Bajotto G, Oshida Y, Sato Y. Cinnamon extract (traditional herb) potentiates in vivo insulin-regulated glucose utilization via enhancing insulin signaling in rats. Diabetes Res Clin Pract 2003; 62: 139–48.
4. Ziegenfuss TN, Hofheins JE, Mendel RW, Landis J, Anderson RA. Effects of a water-soluble cinnamon extract on body composition and features of the metabolic syndrome in pre-diabetic men and women. J Int Soc Sports Nutr 2006; 3: 45–53.
5. Blakytny R, Jude EB. Altered molecular mechanisms of diabetic foot ulcers. Int J Low Extrem Wounds 2009; 8: 95–104.
6. Cavanagh PR, Lipsky BA, Bradbury AW, Botek G. Treatment for diabetic foot ulcers. Lancet 2005; 366: 1725–35.
7. Muniyappa R, Iantorno M, Quon MJ. An integrated view of insulin resistance and endothelial dysfunction. Endocrinol Metab Clin North Am 2008; 37: 685–711, ix–x.
8. Hurlin PJ, Kaur P, Smith PP, Perez-Reyes N, Blanton RA, McDougall JK. Progression of human papillomavirus type 18-immortalized human keratinocytes to a malignant phenotype. Proc Natl Acad Sci USA 1991; 88: 570–4.
9. Panickar KS, Polansky MM, Anderson RA. Cinnamon polyphenols attenuate cell swelling and mitochondrial dysfunction following oxygen-glucose deprivation in glial cells. Exp Neurol 2009; 216: 420–7.
10. Schoene NW, Kelly MA, Polansky MM, Anderson RA. Water-soluble polymeric polyphenols from cinnamon inhibit proliferation and alter cell cycle distribution patterns of hematologic tumor cell lines. Cancer Lett 2005; 230: 134–40.

11. Cao H, Polansky MM, Anderson RA. Cinnamon extract and polyphenols affect the expression of tristetraprolin, insulin receptor, and glucose transporter 4 in mouse 3T3-L1 adipocytes. Arch Biochem Biophys 2007; 459: 214–22.
12. Cao H, Urban JF, Jr, Anderson RA. Cinnamon polyphenol extract affects immune responses by regulating anti- and proinflammatory and glucose transporter gene expression in mouse macrophages. J Nutr 2008; 138: 833–40.
13. Cao H, Urban JF, Jr, Anderson RA. Insulin increases tristetraprolin and decreases VEGF gene expression in mouse 3T3-L1 adipocytes. Obesity (Silver Spring) 2008; 16: 1208–18.
14. Cao H, Graves DJ, Anderson RA. Cinnamon extract regulates glucose transporter and insulin-signaling gene expression in mouse adipocytes. Phytomedicine 2010; 17: 1027–32.
15. Javerzat S, Auguste P, Bikfalvi A. The role of fibroblast growth factors in vascular development. Trends Mol Med 2002; 8: 483–9.
16. Fahey TJ 3rd., Sadaty A, Jones WG, 2nd., Barber A, Smoller B, Shires GT. Diabetes impairs the late inflammatory response to wound healing. J Surg Res 1991; 50: 308–13.
17. Galkowska H, Wojewodzka U, Olszewski WL. Chemokines, cytokines, and growth factors in keratinocytes and dermal endothelial cells in the margin of chronic diabetic foot ulcers. Wound Repair Regen 2006; 14: 558–65.
18. Roberts AB. Transforming growth factor-beta: activity and efficacy in animal models of wound healing. Wound Repair Regen 1995; 3: 408–18.
19. Klass BR, Grobbelaar AO, Rolfe KJ. Transforming growth factor beta1 signalling, wound healing and repair: a multifunctional cytokine with clinical implications for wound repair, a delicate balance. Postgrad Med J 2009; 85: 9–14.
20. Lobmann R, Ambrosch A, Schultz G, Waldmann K, Schiweck S, Lehnert H. Expression of matrix-metalloproteinases and their inhibitors in the wounds of diabetic and non-diabetic patients. Diabetologia 2002; 45: 1011–6.
21. Ke Q, Costa M. Hypoxia-inducible factor-1 (HIF-1). Mol Pharmacol 2006; 70: 1469–80.
22. Lee JW, Bae SH, Jeong JW, Kim SH, Kim KW. Hypoxia-inducible factor (HIF-1)alpha: its protein stability and biological functions. Exp Mol Med 2004; 36: 1–12.
23. Drexler H. Endothelial dysfunction: clinical implications. Prog Cardiovasc Dis 1997; 39: 287–324.
24. Radomski MW, Palmer RM, Moncada S. The role of nitric oxide and cGMP in platelet adhesion to vascular endothelium. Biochem Biophys Res Commun 1987; 148: 1482–9.
25. Sarkar R, Meinberg EG, Stanley JC, Gordon D, Webb RC. Nitric oxide reversibly inhibits the migration of cultured vascular smooth muscle cells. Circ Res 1996; 78: 225–30.
26. Kubes P, Suzuki M, Granger DN. Nitric oxide: an endogenous modulator of leukocyte adhesion. Proc Natl Acad Sci USA 1991; 88: 4651–5.
27. Montagnani M, Golovchenko I, Kim I, Koh GY, Goalstone ML, Mundhekar AN, et al. Inhibition of phosphatidylinositol 3-kinase enhances mitogenic actions of insulin in endothelial cells. J Biol Chem 2002; 277: 1794–9.
28. Mukai Y, Wang CY, Rikitake Y, Liao JK. Phosphatidylinositol 3-kinase/protein kinase Akt negatively regulates plasminogen activator inhibitor type 1 expression in vascular endothelial cells. Am J Physiol Heart Circ Physiol 2007; 292: H1937–42.

***Tom Karagiannis**
Epigenomic Medicine
BakerIDI Heart and Diabetes Institute
75 Commercial Road
Melbourne,VIC.
Australia
Tel: +613 8532 1309
Fax: +613 8532 1100
Email: tom.karagiannis@bakeridi.edu.au

Citation: Pathobiology of Aging & Age-related Diseases 2012, **2**: 11905 - DOI: 10.3402/pba.v2i0.11905